World Journal of Radiology

Online Submissions: http://www.wjgnet.com/1949-8470office
wjr@wjgnet.com
doi:10.4329/wjr.v4.i1.1

World J Radiol 2012 January 28; 4(1): 1-12
ISSN 1949-8470 (online)

EDITORIAL

Value of MR contrast media in image-guided body interventions

Maythem Saeed, Mark Wilson

Maythem Saeed, Mark Wilson, Department of Radiology and Biomedical Imaging, University of California San Francisco, San Francisco, CA 94107-5705, United States
Author contributions: Saeed M contributed to the conception and design, acquisition of data, drafting the article, writing and revising it critically for intellectual content; Wilson M contributed to the acquisition of data, revising the article critically for intellectual content and approving the final version.
Correspondence to: Maythem Saeed, Professor of Radiology and Biomedical Imaging, Department of Radiology and Biomedical Imaging, University of California San Francisco, 185 Berry Street, Suite 350, Campus Box 0946, San Francisco, CA 94107-5705, United States. maythem.saeed@ucsf.edu
Telephone: +1-415-5146221 Fax: +1-415-3539423
Received: August 6, 2011 Revised: October 28, 2011
Accepted: November 4, 2011
Published online: January 28, 2012

Abstract

In the past few years, there have been multiple advances in magnetic resonance (MR) instrumentation, *in vivo* devices, real-time imaging sequences and interventional procedures with new therapies. More recently, interventionists have started to use minimally invasive image-guided procedures and local therapies, which reduce the pain from conventional surgery and increase drug effectiveness, respectively. Local therapy also reduces the systemic dose and eliminates the toxic side effects of some drugs to other organs. The success of MR-guided procedures depends on visualization of the targets in 3D and precise deployment of ablation catheters, local therapies and devices. MR contrast media provide a wealth of tissue contrast and allows 3D and 4D image acquisitions. After the development of fast imaging sequences, the clinical applications of MR contrast media have been substantially expanded to include pre- during- and post-interventions. Prior to intervention, MR contrast media have the potential to localize and delineate pathologic tissues of vital organs, such as the brain, heart, breast, kidney, prostate, liver and uterus. They also offer other options such as labeling therapeutic agents or cells. During intervention, these agents have the capability to map blood vessels and enhance the contrast between the endovascular guidewire/catheters/devices, blood and tissues as well as direct therapies to the target. Furthermore, labeling therapeutic agents or cells aids in visualizing their delivery sites and tracking their tissue distribution. After intervention, MR contrast media have been used for assessing the efficacy of ablation and therapies. It should be noted that most image-guided procedures are under preclinical research and development. It can be concluded that MR contrast media have great value in preclinical and some clinical interventional procedures. Future applications of MR contrast media in image-guided procedures depend on their safety, tolerability, tissue specificity and effectiveness in demonstrating success of the interventions and therapies.

Key words: Magnetic resonance imaging; Contrast media; Magnetic resonance-guided interventions; Tissue ablation; Local therapy

Peer reviewers: Yahya Paksoy, MD, Professor, Department of Radiology, Selcuk University Meram Chool of Medicine, 42085 Konya, Turkey; Dr. Monvadi Barbara Srichai-Parsia, Department of Radiology and Medicine, NYU School of Medicine, 530 First Avenue, HCC-C48, New York 11211, United States

Saeed M, Wilson M. Value of MR contrast media in image-guided body interventions. *World J Radiol* 2012; 4(1): 1-12 Available from: URL: http://www.wjgnet.com/1949-8470/full/v4/i1/1.htm DOI: http://dx.doi.org/10.4329/wjr.v4.i1.1

INTRODUCTION

Image-guided procedures are a minimally invasive form of treatment for diseased vessels and organs. Catheters, devices and therapies are introduced into internal organs *via* different routes and can be guided by real-time

imaging. Image-guided procedures are consequently less invasive than surgical procedures and demonstrate similar patient outcomes[1]. Recent percutaneous intervention studies showed steady increase in the usage of contrast media. Iodinated contrast media are routinely utilized in procedures guided by X-ray fluoroscopy and computed tomography, but these agents have nephrotoxic effects and require ionizing radiation to be visualized, which elevates cancer risk[2,3].

In the early 1980 magnetic resonance (MR) contrast media were introduced. MR contrast media exhibit paramagnetic properties that lead to contrast enhancement by shortening the longitudinal (T_1) or transverse (T_2) relaxation times. These agents rapidly pass to the extracellular compartment and are quickly eliminated by glomerular filtration. Unlike iodinated contrast media, they do not require ionizing radiation to be visualized. These agents are pivotal for accurate disease detection, pathology characterization and treatment planning. MR contrast media provide a wealth of tissue contrast that can be manipulated by the acquisition sequences. Refinements in imaging sequences can reduce the required dose of MR contrast media. This editorial summarizes the important applications of MR contrast media in MR-guided interventions and therapies.

MR CONTRAST MEDIA

MR contrast media represent alternative diagnostic options in patients at risk for adverse reactions to iodinated contrast media. In the early phase of using MR contrast media, the main problem was their toxicity because investigators used pure paramagnetic heavy metal ions. Later paramagnetic ions were chelated with DTPA, DOTA or BOPTA to reduce their toxicity. The chelation, however, reduced some of the paramagnetic properties of free ions. MR contrast media improve diagnostic accuracy, tissue contrast and visibility of inflammation, necrosis, tumor and vascular plaques.

In the late 1980 and early 1990 the first gadolinium-chelate was approved for clinical routine. Currently, the FDA has approved several extracellular gadolinium-chelates and only one gadolinium-based intravascular agent (gadofosveset trisodium)[4]. Other preclinical gadolinium-based intravascular media, which are used to extract physiologic and morphologic information are Gadomer 17[5] and P792[6]. Extravasation and elimination of intravascular contrast media are very slow compared with extracellular contrast media.

In general extracellular gadolinium chelate and blood pool iron oxide particle MR contrast media have been safely and successfully used in patients. In 2005 the observation of nephrogenic systemic fibrosis (NSF), however, cautioned the handling of gadolinium-based MR contrast media[7,8]. NSF describes a systemic body collagenosis, most likely evoked by the deposition of gadolinium ions in the tissue. NSF was observed in patients with reduced renal function (eGFR < 30 mL/min) after the repeated injection of high doses of gadolinium-chelates[7]. Besides the dose, the chemical structure of the chelate (defining the complex stability) has a major impact in increasing the risk of developing NSF. Thus, there is a strong need to minimize the dose of MR contrast media, especially in interventional procedures, where patients are subjected to repeated contrast injections.

Classification of MR contrast media is based on: (1) their distribution in the tissue compartments, namely the extracellular compartment (low molecular weight; < 2 kDa), intravascular compartment (high molecular weight; > 50 kDa), or intracellular compartment or (2) their effects on longitudinal (T_1), transverse (T_2) relaxation times and susceptibility shift (T_2*) of tissues and thereby change tissue signal intensity[9,10]. While T_1 shortening increases signal intensity, T_2 shortening does the opposite. Extracellular or low molecular weight MR contrast media were widely used in interventional procedures, while intravascular or high molecular weight media, such as iron oxide particles, were used for cell labeling.

Iron oxide particles have been used as T1 and T2* MR contrast media to increase and decrease signal intensity of the region of interest on magnetic resonance imaging (MRI). Due to their size and composition, the particles remain in the intravascular compartment for a prolonged period. This class of agents has a high safety index and is not associated with NSF. There are two types of iron particles: (1) superparamagnetic iron oxide particles; and (2) ultrasmall superparamagnetic iron oxide particles. These agents are promising since their properties can be tuned for specific applications, such as cell labeling, drug targeting[11-13], tissue ablation[14] and cancer therapy[15]. They have also become MR markers of inflammatory and degenerative disorders associated with a high macrophage phagocytic activity[16].

APPLICATIONS OF MR CONTRAST MEDIA IN BODY INTERVENTIONS

Endovascular catheters and devices

A considerable research effort is directed at improving the detection of vascular disease with different imaging modalities, such as X-ray, computed tomography, intravascular ultrasound and MR angiography. Because of lack of harmful radiation and high soft tissue contrast, MR angiography is considered the most patient-friendly among these techniques. The main challenge for MR angiography is derived from the fact that the signal originates from water protons, which are abundant in the body. Inevitably, this leads to a background signal in the image and the blood pool cannot exclusively be seen.

Clinical and experimental studies showed that contrast enhanced MR angiography is possible for a selective and exclusive visualization of the vasculature. Delivering MR contrast media during catheter navigation can reduce image blurring and artifacts resulting from the movement of flowing blood, which allows for reaching the steady state earlier. Endovascular catheters and devices appear as dark objects in these cases. Furthermore, intravenous

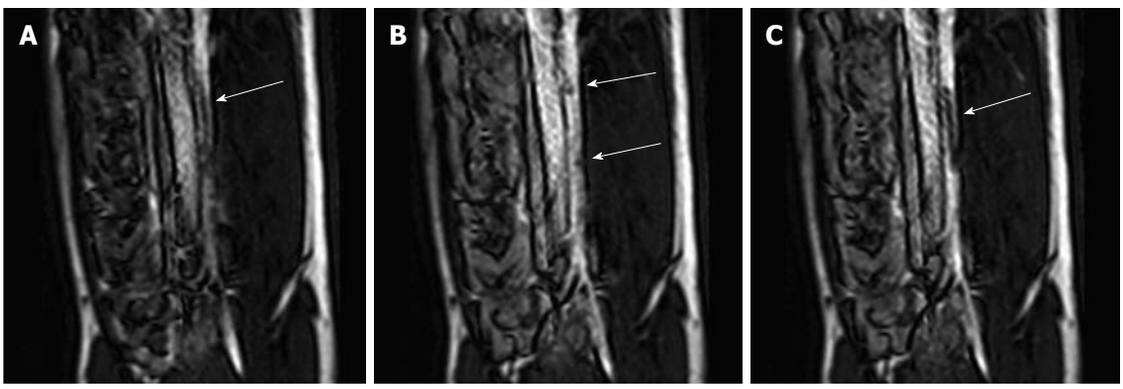

Figure 1 Selected magnetic resonance-guided images of the abdominal aorta prior to the administration of intravascular gadolinium-based (T1 enhancing agent) magnetic resonance contrast medium, the inflated balloon on the catheter is evident (arrow), but suffers substantial downstream signal loss (A). After a blood pool magnetic resonance (MR) contrast medium administration (B), the MR dysprosium-chelate (markers placed on the catheter shaft) becomes evident (arrows, B) and, following inflation, the spatial extent of the balloon is better delineated (arrow, C).

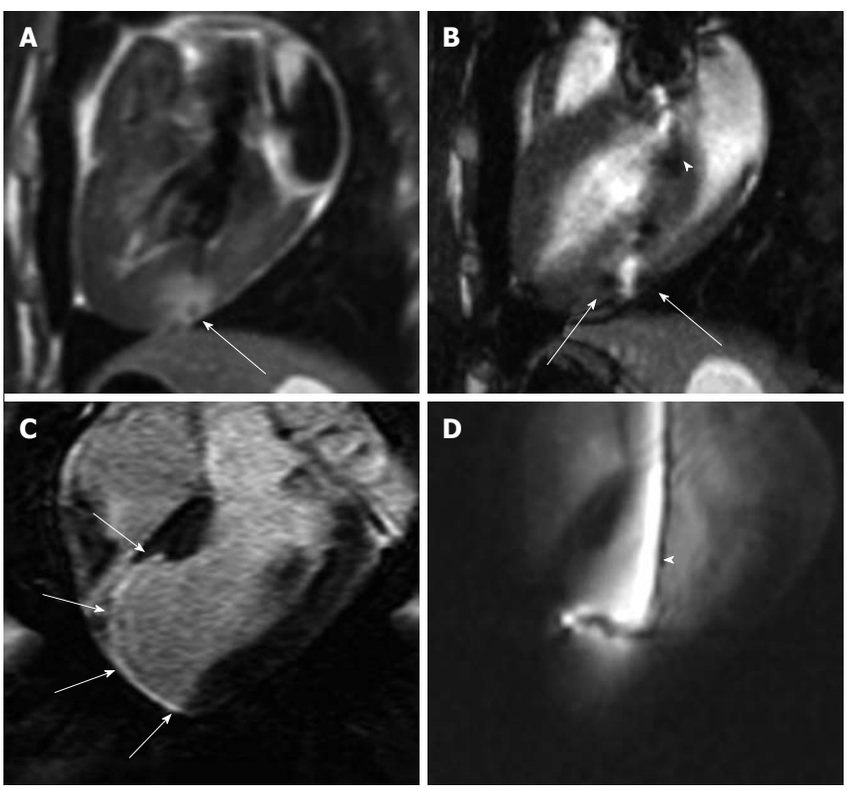

Figure 2 Gadolinium-based magnetic resonance contrast media (T1 enhancing agent) have been used for multiple purposes in cardiac interventions. A: These agents (at a low concentration) have been used to create a target in the myocardium; B: Gadolinium oxide powder was used to coat the endovascular catheter to facilitate navigation into the LV (white arrowhead); C: Magnetic resonance (MR) contrast medium was also used for enhancing and measuring the target (myocardial infarct) (white arrows); D: Selected MR-guided images show an active catheter hitting the infarcted target.

injection of MR contrast media during vascular intervention ensures procedure safety by enhancing the contrast between the vascular wall and endovascular catheter[17] (Figure 1) and may prevent vascular perforation[18]. Investigators coated the shaft and tip of endovascular catheters with either T_2* or T_1[19,20] MR contrast media to enhance the contrast between the blood pool and endovascular catheter, in which the devices appear either hypoenhanced or hyperenhanced based on the sequence and contrast media.

Defining targets

A central challenge for the field of local therapy in tumors and cardiovascular diseases is the capability to visualize the catheter, target and targeting penumbra. MR contrast media showed promising results in visualizing, sizing and targeting penumbra (Figure 2), thereby allowing the interventionalists to determine the dose of the therapy based on size of the pathology. Furthermore, mixing MR contrast media with therapies may assist in ensuring tissue delivery and track its distribution over

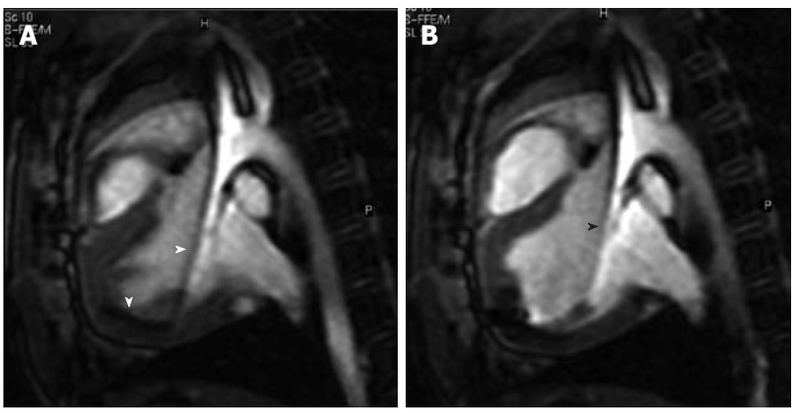

Figure 3 Selected magnetic resonance-guided images showing the advancement of a passive injecting catheter (arrowheads) in the left ventricle prior to (A) and after injecting dysprosium-chelate (T2* enhancing agent) magnetic resonance contrast medium (B, arrowhead) to ensure delivery in the targeted myocardium.

time (Figures 2 and 3).

MR contrast media are useful in evaluating the efficacy of therapy by allowing the determination of tissue perfusion, blood volume, vascular permeability, angiogenesis and cellular integrity[21,22]. For example, after effective chemotherapy there is a decrease in the size of the lesion and number of microvessels, which can be detected on contrast enhanced MR images.

Body Interventions

Transcatheter embolization of the uterine arteries for treatment of uterine fibroids was introduced 1995 in France and has been performed in the United States since 1996. This technique is currently used for treatment of symptomatic uterine fibroids[23] and hepatocellular tumors[24]. The standard protocol for evaluation of this intervention consists of dynamic gadolinium-enhanced 3D pelvic MR angiography and delayed contrast enhanced MRI[25]. Prior to transcatheter embolization of the uterine arteries, contrast enhanced MRI is performed to confirm the diagnosis, map (determine the size, number and location of the pathology), predict treatment response (high signal intensity associated with poor response) and roadmap the pelvic vasculature[26]. Embolization follow up showed that the procedure was successful when fibroids were unenhanced and the uterine arteries were invisible on perfusion MRI[27]. In a rabbit tumor model, Chung *et al*[28] used intra-arterial bolus injection of gadolinium-based MR contrast medium to measure uterine fibroid perfusion before and after uterine artery embolization. After positioning a catheter within the uterine artery and injecting the microemboli, they found that uterine tumor perfusion decreased by 76% on MRI. Others found that patchy perfusion suggests incomplete uterine artery occlusion and treatment failure[29,30]. This contrast enhanced MRI technique could be used to determine an optimal embolic endpoint with the long-term goals of improving uterine artery embolization success rates and minimizing procedure-related ischemic pain.

A major limitation of transcatheter arterial embolization is the inability to image and determine the *in vivo* fate of the injected emboli. Assessment of embolization relies on interpretation of visual blood flow information[23,31] and operator inferences. The limitations of transcatheter arterial embolization were demonstrated in a study probing the perceived and real completeness of uterine fibroid embolization. Investigators found incomplete embolization in 20% of cases despite indications by angiography of complete occlusion. They also found that incomplete embolization of uterine fibroids has led to tumor recurrence and persistence of symptoms[32], while exceeding the endpoint by injecting too much embolic material increases the chances of uterine damage[31]. Until recently, there has been no noninvasive technique to track/map the distribution of embolic materials after intervention, which represents a significant disadvantage. Therefore, Fidelman *et al*[33] impregnated the embolic materials (300-500 and 500-700 μm in diameters) with gadolinium-chelate by diffusion of the contrast medium into the core of the porous particles to visualize their distribution. Wilson *et al*[34] used these impregnated embolic materials in visualizing the obstruction of different diameter blood vessels in the kidneys. These materials provided wave-front renal enhancement for > 1 h after injection. Large microemboli preferentially deposited in the medulla, while small microemboli deposited in the cortex. Renal blood flow was significantly reduced after the administration of 300-500 μm microspheres (from 3.9 to 1.0 mL/min per gram) and 500-700 μm microspheres (from 3.5 to 0.2 mL/min per gram)[34] (Figure 4).

In 2008, Cilliers *et al*[35] synthesized and characterized polyvinyl alcohol embolic particles modified with a clinically approved gadolinium-chelate MR contrast media. The investigators used these particles during transcatheter arterial embolization procedures. The polyvinyl alcohol particles are injected into tumor vessels and prevent blood flow, which results in tumor attenuation. They found that MRI of embolic particles facilitate determination of the endpoint of embolization, observe nontarget embolization, and improve the success rate of the procedure.

In 2011, Bartling *et al*[36] presented embolization con-

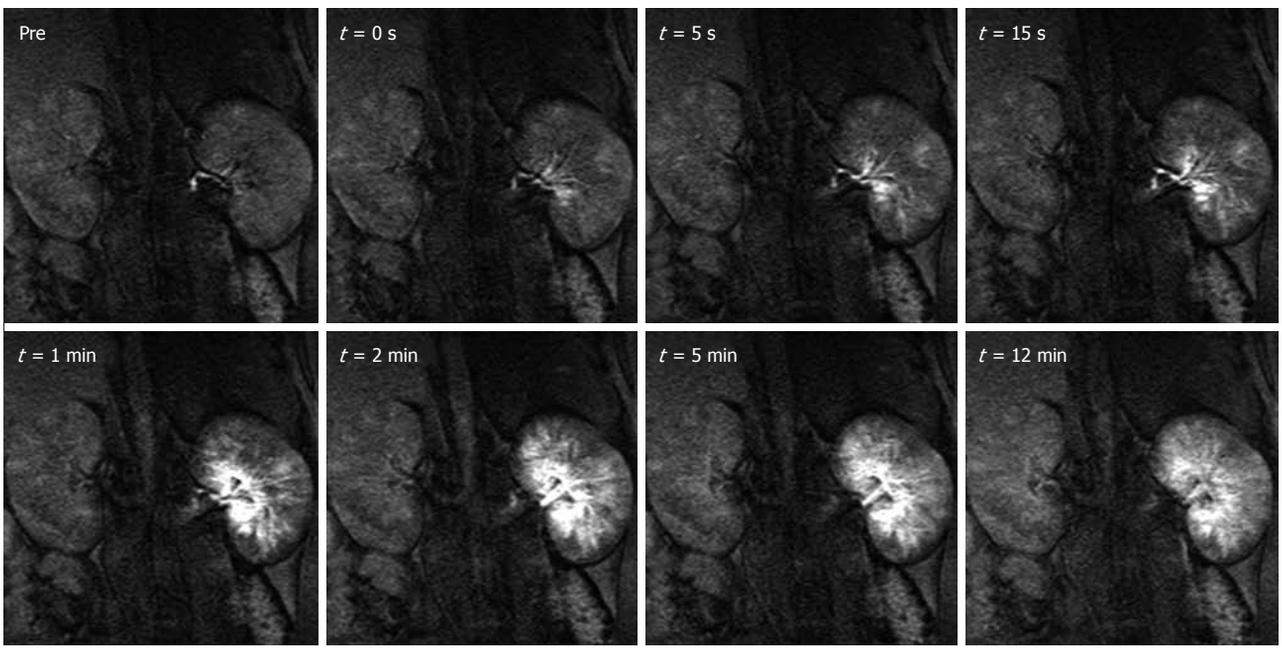

Figure 4 Distribution of magnetic resonance labeled embolic materials as a function of time in the left kidney. Gadolinium-impregnated microspheres caused a steep increase in signal intensity over the cortical and medullary regions. Less than 5 min after the injection, as excess free gadolinium was excreted in the urine, the signal intensities began to decrease but still remained substantially above baseline for both particle sizes. Administration of magnetic resonance contrast media after the procedure confirmed the hypothesis that the injection of microspheres halts blood flow to targeted tissues. Hyperenhanced foci corresponding to microsphere location persisted for at least 1hr after injections. The smaller particles tended to settle more peripherally in the renal cortex, whereas the larger microspheres were lodged in the inner cortical and medullary regions. This new labeling technique may be useful for embolotherapy procedures, such as uterine fibroid embolization, hepatic tumor embolization, and preoperative meningioma embolization.

trast media with a property of being visible on MRI and X-ray/computed tomography, namely iodine and iron particles. They proposed that implementation of this new material in clinical radiology will provide optimization of embolization procedures with regard to prevention of particle misplacement and direct intraprocedural visualization, while improving follow-up examinations by utilizing the complementary characteristics of CT and MRI.

An important clinical application of MR contrast media is that shown by Wilson *et al*[34], where patients with inoperable hepatocellular carcinoma were successfully treated using iron particles bound to doxorubicin. The particles ranged from 0.5-5.0 μm in diameter and were able to leave the vasculature under the influence of the force provided by the external magnet. Once the particles are outside the vasculature, doxorubicin desorbs from them, resulting in a local response with no systemic toxicity. Figures 5 and 6 show the setting of this clinical trial. Drug-bound iron particles can be precisely directed to selective organs by placement of an external magnet. In this study, MR contrast media showed the need for more therapy because of the lack of coverage of the entire tumor in the initial administration. MR images obtained after each dose of the chemotherapeutic agent showed increasing areas of signal intensity loss due to a magnetic susceptibility artifact caused by the iron.

Tissue ablation

Thermal ablation therapies (radiofrequency ablation, interstitial laser thermotherapy, microwave, cryotherapy and high-intensity focused ultrasound) are minimally invasive or non-invasive alternatives to conventional surgical resection. Ablation has been widely implemented in treating arrhythmia in the heart and tumors in the prostate, lung, liver, kidneys, *etc*. Contrast enhanced MRI has been successfully used to assess the success of ablation[37-39]. The diagnostic benefits of MR contrast media in differentiating ablated from non-ablated tissue have been confirmed in multiple centers[40,41]. Prior to the administration of MR contrast media, the appearance of thermally ablated tissue varies between hypointense, isointense and hyperintense. After ablation, MR contrast media provide moderate to intense enhancement of the rim surrounding the thermally ablated tissue. In a prostate cancer study, RFA ablated lesions appear hypoenhanced after gadolinium injection[42]. Similarly, Goldberg and Dupuy observed a lack of contrast enhancement after gadolinium injection in ablated liver metastasis[43]. Accordingly, changes in signal intensity, size, and internal contours of ablated tissue on contrast enhanced MRI gives important clues about the success of therapy[44].

Contrast enhanced MRI is also useful for arrhythmic substrate identification[45,46]. This technique has the ability to encompass the target volume through direct imaging of signal enhancement after tissue ablation in patients[47]. Clinical studies have demonstrated the association between infarct scar, peri-infarcted zone and the risk of monomorphic ventricular tachycardia[46,48,49]. An integrated 3D scar reconstruction from delayed gadolinium-enhanced MRI was used to facilitate ventricular tachycar-

Magneticlly targeted carrier (MTC-DOX)
1-2 μm Fe-activated carbon complexes bound to doxorubicin
Delivered through arterial catheter
Drawn into tissue by portable external magnet
Readily visible on MRI (Fe susceptibiliy artifact)

5 kgauss
samll
(2" × 2.5")
permanent
magnet

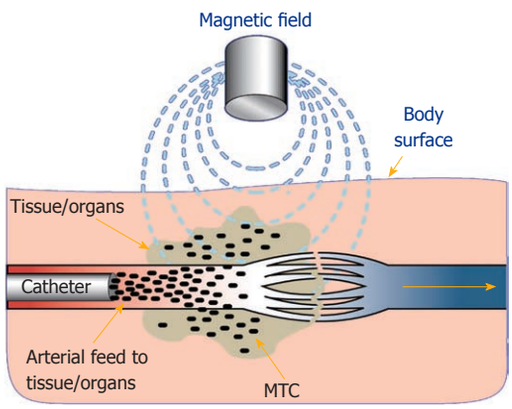

Figure 5 This figure shows a portable magnet (left) and a diagram (right) depicts the mode of action of magnetic targeted therapy in the target. The overall height of the magnet and holding apparatus is 1.4 m. The intra-arterial injected magnetic targeted carrier (iron particles) bound to doxorubicin (MTC-DOX), which is drawn out of the artery into surrounding tumor and/or liver tissue by the influence of the local magnetic field (Image courtesy of FeRx.). MRI: Magnetic resonance imaging.

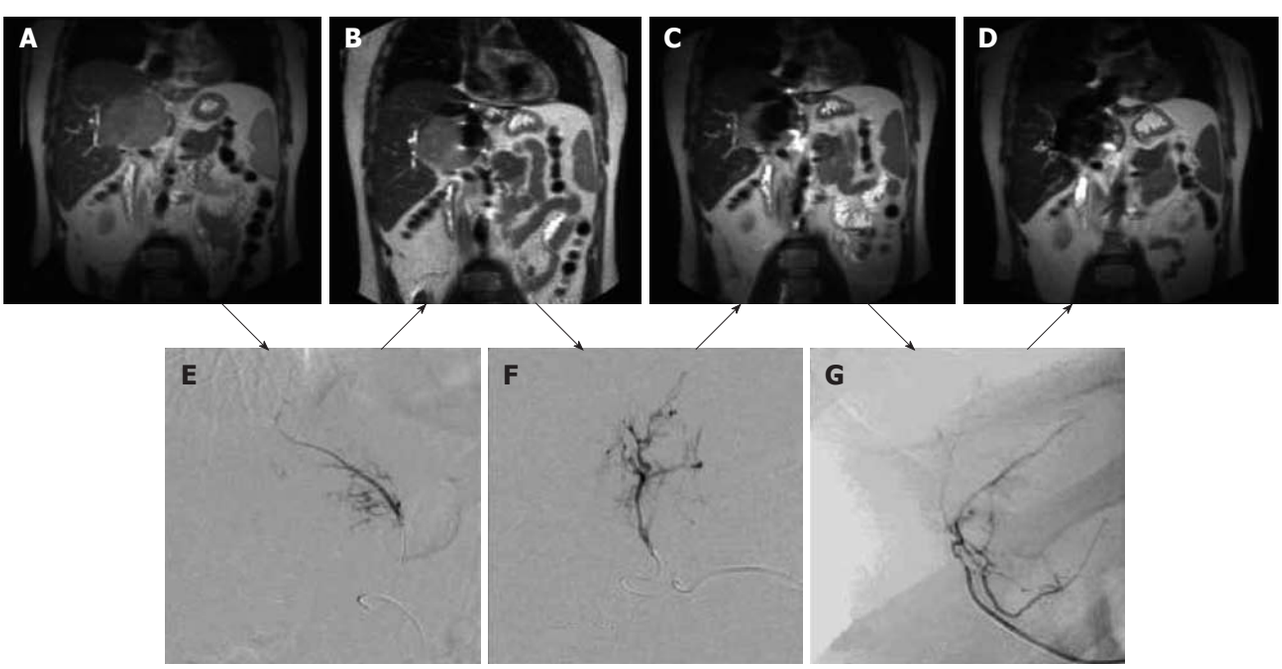

Figure 6 Coronal magnetic resonance images of large hepatocellular carcinoma obtained before magnetic targeted carrier bound to doxorubicin administration (A) and after the first (B), second (C) and third (D) dose of magnetic targeted carrier bound to doxorubicin. The selective hepatic arterial catheter was repositioned between each dose. The initial DSA image (E) was obtained during the injection of magnetic targeted carrier bound to doxorubicin (MTC-DOX) into the left hepatic artery supplying the tumor. The next dose was injected into the hepatic artery branch segment (F), while the third dose was injected into a branch of the right hepatic artery (G). As a result, progressively larger areas of the tumor were affected by MTC-DOX, as documented by the progressive loss of signal intensity due to iron susceptibility artifacts (T_2*) on the intra-procedural coronal magnetic resonance images obtained after each injection.

dia ablation[50]. van Dockum *et al*[51] evaluated myocardial infarction induced by percutaneous transluminal septal myocardial ablation in symptomatic patients with hypertrophic obstructive cardiomyopathy using contrast-enhanced MRI.

Device deployment

A recent experimental study showed the value of MR contrast media in providing diagnostic information on an atrial septal defect, a congenital heart defect in which the wall that separates the atria does not close completely. Schalla *et al*[52] found in an experimental study that gadolinium-filled balloon sizing is a useful method for detecting and sizing the atrial septal defects. They also used MR contrast media to demonstrate intracardiac left-to-right shunt prior to the placement of atrial septal defect device

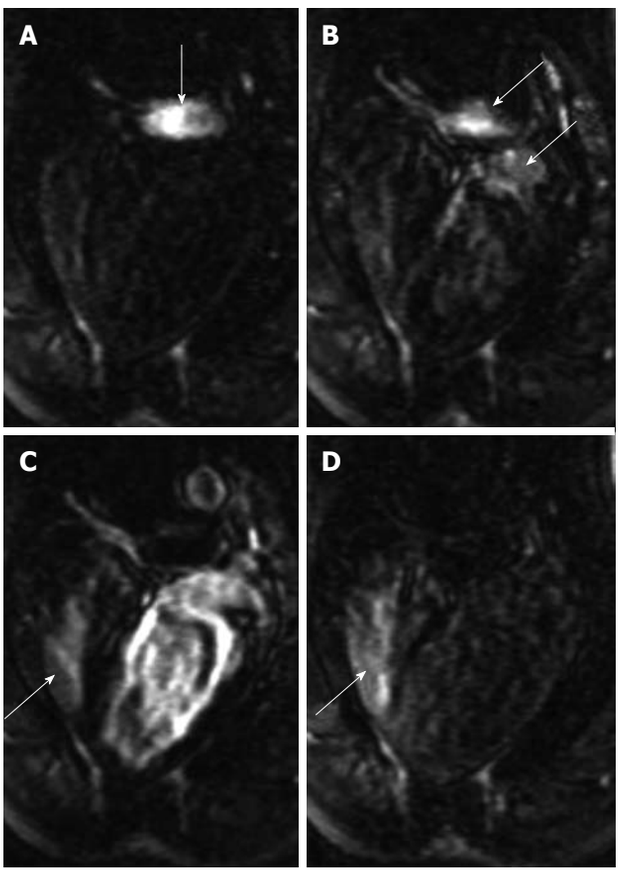

Figure 7 Bolus administration of gadolinium-chelate demonstrates atrial septal defect on cardiac magnetic resonance four-chamber view images. At the time of administration of the contrast medium, the right atrium was enhanced (A, arrow). Images acquired 1-2 s later show the contrast medium in both the pulmonary artery and left atrium (B, arrows) and subsequently in both right (arrow) and left ventricles (C). As a sign of an intracardiac left-to-right shunt, enhancement of the right ventricle is detected simultaneously with enhancement of the left ventricle. The re-enhancement of the right ventricle (D, arrow) as a result of recirculation of the contrast medium was acquired 12 s after image A.

closure, where contrast enhancement of the right ventricle is detected simultaneously with enhancement of the LV (Figure 7).

Therapy

Transendocardial and transvascular routes have been recently used to deliver MR labeled gene and cell therapies. The advantages of labeled therapies are: (1) targeting only pathologic regions; (2) delivering effective doses; and (3) reducing systemic side effects compared with IV injection[53-55]. Unlike intramyocardial injection, intracoronary artery injection of stem cells causes microinfarct, which was confirmed by increase in serum troponin I concentration and electrophysiologic abnormalities detected on electrocardiogram[56]. Recent MR and MDCT studies showed the effectiveness of MR and CT contrast media in detecting and measuring microinfarct size[57,58].

MR contrast media showed great promise in detecting specific biological processes involved in the initiation and progression of atherosclerosis that may require intravascular intervention[59,60]. von Bary *et al*[61] experimentally demonstrated the feasibility of noninvasive assessment of coronary remodeling, using elastin-binding gadolinium. Such data could facilitate the interpretation of clinical findings, enhance risk stratification and provide a means for local therapy. Monitoring extracellular matrix changes by contrast-enhanced MRI appears promising for the assessment of plaque burden in atherosclerosis or neointimal hyperplasia after coronary angioplasty and other therapies[62].

MR contrast media have also been used in quantifying the sizes of the area at risk, myocardial infarct and visualizing therapeutic delivery in the target. Saeed *et al*[63] used MR contrast media in measuring ischemic and infarcted myocardium prior to and after transendocardial delivery of hepatocyte growth factor gene and endothelial growth factor gene using MR-guided procedures. They found that gene treated animals have better perfusion and significantly smaller infarct size than control animals on contrast enhanced MRI (Figure 8).

MR contrast media have also been used to label cells in order to track their distribution in myocardium after intramyocardial injection under MR-guidance[64] or intracoronary infusion[65,66]. Graham *et al*[66] were able to follow the distribution of iron oxide labeled bone marrow progenitor cells for 42 d after intracoronary infusion. The transendocardial delivery route has been shown to be safe in patients with end-stage heart failure[67]. Recent preclinical and clinical studies showed the importance of MR contrast media in determining the efficacy of stem cells[68-70]. First pass MR contrast media passage documented the benefits of angiogenic growth factors[71] and angiogenic genes[72] in increasing regional myocardial perfusion (Figure 9). Pearlman *et al*[71] were the first to demonstrate the recruitment of collateral vessels after local delivery of angiogenic genes, using perfusion MRI.

Angiography

Visualization of vascular anatomy, pathology (stenosis, aneurism, plaque) or implants (stents, filters, atrio-septal occluders or prosthetic heart valves) is crucial in interventional procedures. MR contrast media have been used in road mapping blood vessels[73,74], demonstrating vascular diseases and easing visualization of endovascular devices[21]. These agents were delivered intravenously or intraarterially to enhance arterial[74,75] or venous vessels[76].

Inflammation is a key process in atherosclerotic progression and has been associated with increased frequency of plaque rupture[77]. Ultrasmall superparamagnetic iron oxide particles have been used in characterizing atherosclerotic plaques from many different perspectives. These agents are effective markers of plaque inflammation. Different plaque tissues can then be characterized based on their enhancement properties[78].

Cell labeling

Both gadolinium and iron oxide based contrast media are useful for labeling different types of cells that assist in cell tracking[79,80]. These agents have no negative effects on cell viability, proliferation or differentiation[81,82]. The toxicity of iron oxide particles is less than free gadolinium because free iron particles released from dead iron

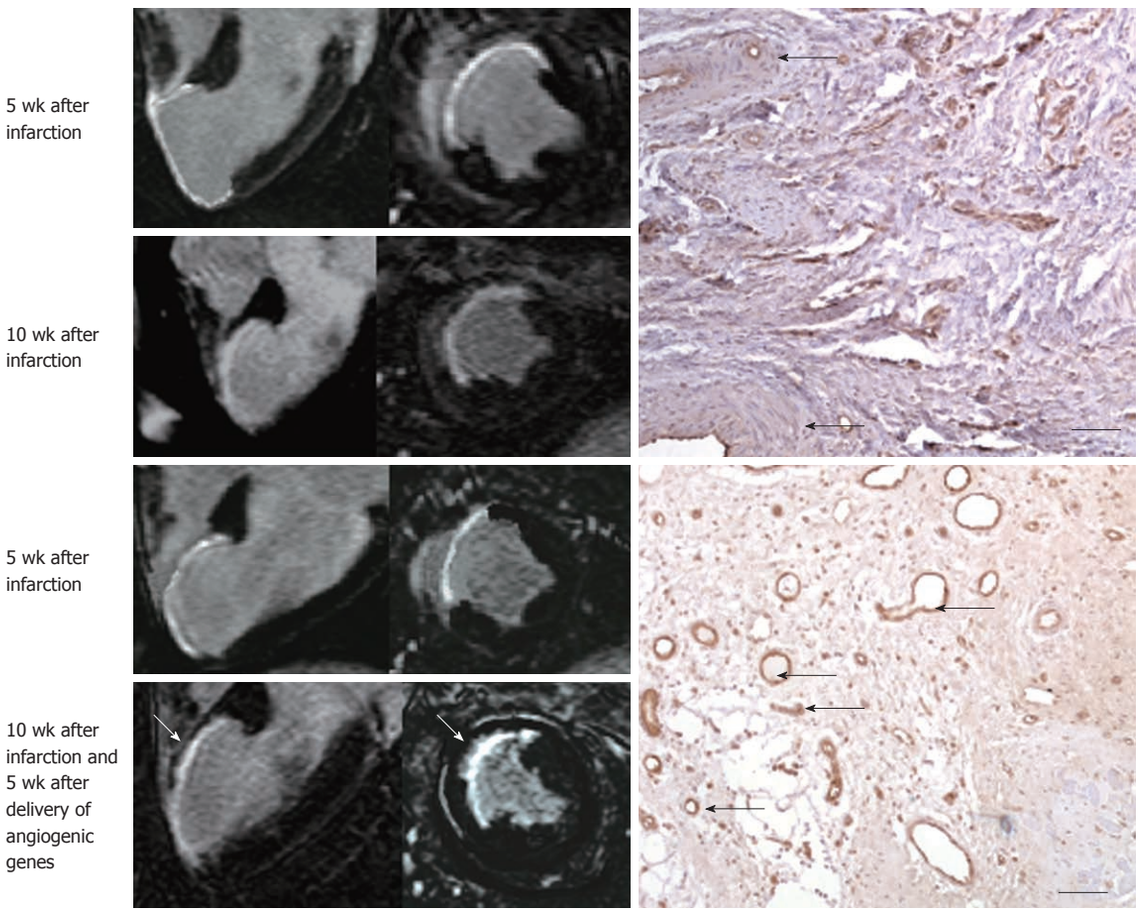

Figure 8 Gadolinium-enhanced magnetic resonance long-axis (left column) and short-axis (right column) images illustrate the extent of myocardial infarct (hyperenhanced myocardium) at 5 wk after infarction and 5 wk after injection of saline (top block, 4 magnetic resonance images) and angiogenic gene (bottom block, 4 magnetic resonance images). Gadolinium-enhanced magnetic resonance (MR) images delineated myocardial infarct and showed substantial reduction in infarct extent and transmurality 5 wk after treatment (bottom block, bottom row, white arrows) compared with control animal (top block, bottom row). The angiogenic gene was delivered transendocardially under MR-guidance as shown in Figure 2. The histopathologic sections (right) show very few blood vessels in control animal (top right, black arrows) and the formation of abundant new blood vessels in gene treated animal (bottom right, black arrows).

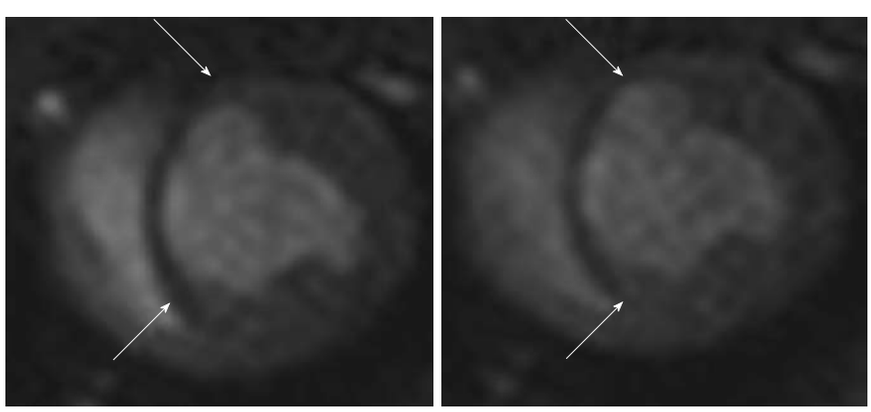

Figure 9 First pass perfusion magnetic resonance imaging shows the hypoperfused infarct scar (arrows) after bolus administration of Gd-DTPA. The magnetic resonance (MR) images illustrate the delay in the enhancement of infarcted myocardium (arrows) compared with remote myocardium. The images were acquired at 12 s (left) and 60 s (right) after bolus administration of MR contrast media.

labeled cells are recycled in the body and not associated with NSF.

MR contrast media can be introduced into the intracellular compartments by endocytosis, phagocytosis or magnetoelectroporation. Investigators found that the duration of detection of labeled cells on MRI varies from 5 wk for embolic stem cells[83] to 16 wk for skeletal myoblasts[84]. Modo *et al*[85] observed that gadolinium chelate labeling allows *in vivo* identification of transplanted neural cells up to 1 year after transplantation in rats with

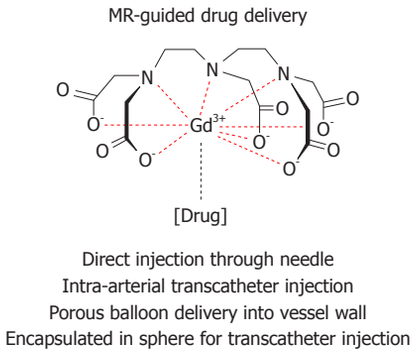

Figure 10 Schematic representation of magnetic resonance labeled therapy and their routes of delivery.

middle cerebral artery occlusion. Bulte *et al*[86] found that the reliable detection limit of a cluster of iron oxide-labeled cells in beating hearts at clinical field strengths is on the order of 100 000 cells. Iron labeling of stem cells generates a hypointense signal (dark region), related to the susceptibility effect of the particles, on T2*-weighted images. Iron oxide particles provide T_2* parametric map for up to 3 wk[79,86,87]. In the future, accurate depiction of treated regions with MR labeled cells may permit rapid adjustments of the therapeutic regimen to improve clinical outcomes.

FUTURE PERSPECTIVES

The usage of MR contrast media in MR guided procedures represents a promising modality, beyond traditional anatomical and functional indices. Figure 10 shows a schematic presentation of MR labeled therapy and their routes of delivery.

Saeed *et al*[21] demonstrated the advantageous effects of vascular endothelial growth factor and hepatocyte growth factor genes, delivered transendocardially under MR-guidance, in creating new blood vessels and reducing the size of infarcted myocardium using gadolinium-based MR contrast media[22]. Others used contrast enhanced MRI for determining the effects of intracoronary stem cell therapy on left ventricular function[88]. The investigators did not observe evidence of positive effects for intracoronary stem cells compared with placebo therapy with respect to left ventricular ejection fraction, volume indexes or infarct size. Other investigators found intracroronary cell delivery cause microinfarction[56]. MR contrast media have been recently used to visualize myocardial microinfarct caused by coronary microemboli[57,58] and in the validation of manual thrombectomy devices[89]. Technical developments in mid-field MR interventional units will lead to reduction of the dose of MR contrast media and result in better visualization of interventional devices.

CONCLUSION

MR contrast media are useful in interventional procedures and therapy evaluation. They allow for characterization of tissue and vascular pathologies. In the follow-up they allow for monitoring of treatment success that is not available on X-ray fluoroscopy and limits the harmful effects of iodinated contrast media. Labeling therapies with MR contrast media may be the future development that will hasten the deployment of effective therapies.

REFERENCES

1 **Chertova E**, Chertov O, Coren LV, Roser JD, Trubey CM, Bess JW, Sowder RC, Barsov E, Hood BL, Fisher RJ, Nagashima K, Conrads TP, Veenstra TD, Lifson JD, Ott DE. Proteomic and biochemical analysis of purified human immunodeficiency virus type 1 produced from infected monocyte-derived macrophages. *J Virol* 2006; **80**: 9039-9052
2 **Wagner LK**, Eifel P, Geise R. Effects of ionizing radiation. *J Vasc Interv Radiol* 1995; **6**: 988-989
3 **Zhou W**, Parent LJ, Wills JW, Resh MD. Identification of a membrane-binding domain within the amino-terminal region of human immunodeficiency virus type 1 Gag protein which interacts with acidic phospholipids. *J Virol* 1994; **68**: 2556-2569
4 **Freed EO**. HIV-1 Gag: flipped out for PI(4,5)P(2). *Proc Natl Acad Sci USA* 2006; **103**: 11101-11102
5 **Saad JS**, Miller J, Tai J, Kim A, Ghanam RH, Summers MF. Structural basis for targeting HIV-1 Gag proteins to the plasma membrane for virus assembly. *Proc Natl Acad Sci USA* 2006; **103**: 11364-11369
6 **Hermida-Matsumoto L**, Resh MD. Human immunodeficiency virus type 1 protease triggers a myristoyl switch that modulates membrane binding of Pr55(gag) and p17MA. *J Virol* 1999; **73**: 1902-1908
7 **Naghavi MH**, Goff SP. Retroviral proteins that interact with the host cell cytoskeleton. *Curr Opin Immunol* 2007; **19**: 402-407
8 **Tomita Y**, Noda T, Fujii K, Watanabe T, Morikawa Y, Kawaoka Y. The cellular factors Vps18 and Mon2 are required for efficient production of infectious HIV-1 particles. *J Virol* 2011; **85**: 5618-5627
9 **Dong X**, Li H, Derdowski A, Ding L, Burnett A, Chen X, Peters TR, Dermody TS, Woodruff E, Wang JJ, Spearman P. AP-3 directs the intracellular trafficking of HIV-1 Gag and plays a key role in particle assembly. *Cell* 2005; **120**: 663-674
10 **Camus G**, Segura-Morales C, Molle D, Lopez-Vergès S, Begon-Pescia C, Cazevieille C, Schu P, Bertrand E, Berlioz-Torrent C, Basyuk E. The clathrin adaptor complex AP-1 binds HIV-1 and MLV Gag and facilitates their budding. *Mol Biol Cell* 2007; **18**: 3193-3203
11 **Parent LJ**. New insights into the nuclear localization of retroviral Gag proteins. *Nucleus* 2011; **2**: 92-97
12 **Dupont S**, Sharova N, DéHoratius C, Virbasius CM, Zhu X, Bukrinskaya AG, Stevenson M, Green MR. A novel nuclear export activity in HIV-1 matrix protein required for viral replication. *Nature* 1999; **402**: 681-685
13 **Jouvenet N**, Bieniasz PD, Simon SM. Imaging the biogenesis of individual HIV-1 virions in live cells. *Nature* 2008; **454**: 236-240
14 **Hadjipanayis CG**, Bonder MJ, Balakrishnan S, Wang X, Mao H, Hadjipanayis GC. Metallic iron nanoparticles for MRI contrast enhancement and local hyperthermia. *Small* 2008; **4**: 1925-1929
15 **Pornillos O**, Ganser-Pornillos BK, Kelly BN, Hua Y, Whitby FG, Stout CD, Sundquist WI, Hill CP, Yeager M. X-ray structures of the hexameric building block of the HIV capsid. *Cell* 2009; **137**: 1282-1292
16 **Cortines JR**, Monroe EB, Kang S, Prevelige PE. A retroviral chimeric capsid protein reveals the role of the N-terminal β-hairpin in mature core assembly. *J Mol Biol* 2011; **410**: 641-652

17 **Paillart JC**, Shehu-Xhilaga M, Marquet R, Mak J. Dimerization of retroviral RNA genomes: an inseparable pair. *Nat Rev Microbiol* 2004; **2**: 461-472

18 **Saeed M**, Henk CB, Weber O, Martin A, Wilson M, Shunk K, Saloner D, Higgins CB. Delivery and assessment of endovascular stents to repair aortic coarctation using MR and X-ray imaging. *J Magn Reson Imaging* 2006; **24**: 371-378

19 **Wyma DJ**, Jiang J, Shi J, Zhou J, Lineberger JE, Miller MD, Aiken C. Coupling of human immunodeficiency virus type 1 fusion to virion maturation: a novel role of the gp41 cytoplasmic tail. *J Virol* 2004; **78**: 3429-3435

20 **Unal O**, Li J, Cheng W, Yu H, Strother CM. MR-visible coatings for endovascular device visualization. *J Magn Reson Imaging* 2006; **23**: 763-769

21 **Saeed M**, Martin A, Jacquier A, Bucknor M, Saloner D, Do L, Ursell P, Su H, Kan YW, Higgins CB. Permanent coronary artery occlusion: cardiovascular MR imaging is platform for percutaneous transendocardial delivery and assessment of gene therapy in canine model. *Radiology* 2008; **249**: 560-571

22 **Zhang H**, Zhao Q, Bhattacharya S, Waheed AA, Tong X, Hong A, Heck S, Curreli F, Goger M, Cowburn D, Freed EO, Debnath AK. A cell-penetrating helical peptide as a potential HIV-1 inhibitor. *J Mol Biol* 2008; **378**: 565-580

23 **Adamson CS**, Freed EO. Novel approaches to inhibiting HIV-1 replication. *Antiviral Res* 2010; **85**: 119-141

24 **Castrucci M**, Sironi S, De Cobelli F, Salvioni M, Del Maschio A. Plain and gadolinium-DTPA-enhanced MR imaging of hepatocellular carcinoma treated with transarterial chemoembolization. *Abdom Imaging* 1996; **21**: 488-494

25 **Mueller GC**, Gemmete JJ, Carlos RC. **Diagnostic imaging** and vascular embolization for uterine leiomyomas. *Semin Reprod Med* 2004; **22**: 131-142

26 **Kelly BN**, Kyere S, Kinde I, Tang C, Howard BR, Robinson H, Sundquist WI, Summers MF, Hill CP. Structure of the antiviral assembly inhibitor CAP-1 complex with the HIV-1 CA protein. *J Mol Biol* 2007; **373**: 355-366

27 **Freed EO**. HIV-1 and the host cell: an intimate association. *Trends Microbiol* 2004; **12**: 170-177

28 **Chung JC**, Wang D, Lewandowski RJ, Tang R, Chrisman HB, Vogelzang RL, Woloschak GE, Larson AC, Omary RA, Ryu RK. Four-dimensional transcatheter intra-arterial perfusion MR imaging before and after uterine artery embolization in the rabbit VX2 tumor model. *J Magn Reson Imaging* 2010; **31:** 1137-1143

29 **Pornillos O**, Alam SL, Davis DR, Sundquist WI. **Structure of** the Tsg101 UEV domain in complex with the PTAP motif of the HIV-1 p6 protein. *Nat Struct Biol* 2002; **9**: 812-817

30 **Liu F**, Stephen AG, Waheed AA, Aman MJ, Freed EO, Fisher RJ, Burke TR. SAR by oxime-containing peptide libraries: application to Tsg101 ligand optimization. *Chembiochem* 2008; **9**: 2000-2004

31 **Huang JY**, Kafy S, Dugas A, Valenti D, Tulandi T. Failure of uterine fibroid embolization. *Fertil Steril* 2006; **85**: 30-35

32 **Dorenberg EJ**, Novakovic Z, Smith HJ, Hafsahl G, Jakobsen JA. Uterine fibroid embolization can still be improved: observations on post-procedure magnetic resonance imaging. *Acta Radiol* 2005; **46**: 547-553

33 **Fidelman N**, Wilson MW, Weber OM, Martin AJ, Kerlan RK, LaBerge JM, Gordon RL. Real-time MR properties of particulate embolic agents tested in a dynamic flow model. *J Vasc Interv Radiol* 2002; **13**: 613-618

34 **Wilson MW**, Fidelman N, Weber OM, Martin AJ, Gordon RL, LaBerge JM, Kerlan RK, Wolanske KA, Saeed M. Experimental renal artery embolization in a combined MR imaging/angiographic unit. *J Vasc Interv Radiol* 2003; **14**: 1169-1175

35 **Cilliers R**, Song Y, Kohlmeir EK, Larson AC, Omary RA, Meade TJ. Modification of embolic-PVA particles with MR contrast agents. *Magn Reson Med* 2008; **59**: 898-902

36 **Bartling SH**, Budjan J, Aviv H, Haneder S, Kraenzlin B, Michaely H, Margel S, Diehl S, Semmler W, Gretz N, Schönberg SO, Sadick M. First multimodal embolization particles visible on x-ray/computed tomography and magnetic resonance imaging. *Invest Radiol* 2011; **46**: 178-186

37 **Carrillo A**, Duerk JL, Lewin JS, Wilson DL. Semiautomatic 3-D image registration as applied to interventional MRI liver cancer treatment. *IEEE Trans Med Imaging* 2000; **19**: 175-185

38 **Quesson B**, de Zwart JA, Moonen CT. Magnetic resonance temperature imaging for guidance of thermotherapy. *J Magn Reson Imaging* 2000; **12**: 525-533

39 **Salomir R**, Vimeux FC, de Zwart JA, Grenier N, Moonen CT. Hyperthermia by MR-guided focused ultrasound: accurate temperature control based on fast MRI and a physical model of local energy deposition and heat conduction. *Magn Reson Med* 2000; **43**: 342-347

40 **Bruix J**, Sherman M, Llovet JM, Beaugrand M, Lencioni R, Burroughs AK, Christensen E, Pagliaro L, Colombo M, Rodés J. Clinical management of hepatocellular carcinoma. Conclusions of the Barcelona-2000 EASL conference. European Association for the Study of the Liver. *J Hepatol* 2001; **35**: 421-430

41 **Forner A**, Ayuso C, Varela M, Rimola J, Hessheimer AJ, de Lope CR, Reig M, Bianchi L, Llovet JM, Bruix J. Evaluation of tumor response after locoregional therapies in hepatocellular carcinoma: are response evaluation criteria in solid tumors reliable? *Cancer* 2009; **115**: 616-623

42 **Djavan B**, Zlotta AR, Susani M, Heinz G, Shariat S, Silverman DE, Schulman CC, Marberger M. Transperineal radiofrequency interstitial tumor ablation of the prostate: correlation of magnetic resonance imaging with histopathologic examination. *Urology* 1997; **50**: 986-992; discussion 992-993

43 **Nahum Goldberg S**, Dupuy DE. **Image-guided radiofrequency** tumor ablation: challenges and opportunities--part I. *J Vasc Interv Radiol* 2001; **12**: 1021-1032

44 **Dromain C**, de Baere T, Elias D, Kuoch V, Ducreux M, Boige V, Petrow P, Roche A, Sigal R. Hepatic tumors treated with percutaneous radio-frequency ablation: CT and MR imaging follow-up. *Radiology* 2002; **223**: 255-262

45 **Babu-Narayan SV**, Goktekin O, Moon JC, Broberg CS, Pantely GA, Pennell DJ, Gatzoulis MA, Kilner PJ. Late gadolinium enhancement cardiovascular magnetic resonance of the systemic right ventricle in adults with previous atrial redirection surgery for transposition of the great arteries. *Circulation* 2005; **111**: 2091-2098

46 **Nazarian S**, Bluemke DA, Lardo AC, Zviman MM, Watkins SP, Dickfeld TL, Meininger GR, Roguin A, Calkins H, Tomaselli GF, Weiss RG, Berger RD, Lima JA, Halperin HR. Magnetic resonance assessment of the substrate for inducible ventricular tachycardia in nonischemic cardiomyopathy. *Circulation* 2005; **112**: 2821-2825

47 **McGann CJ**, Kholmovski EG, Oakes RS, Blauer JJ, Daccarett M, Segerson N, Airey KJ, Akoum N, Fish E, Badger TJ, DiBella EV, Parker D, MacLeod RS, Marrouche NF. New magnetic resonance imaging-based method for defining the extent of left atrial wall injury after the ablation of atrial fibrillation. *J Am Coll Cardiol* 2008; **52**: 1263-1271

48 **Bello D**, Fieno DS, Kim RJ, Pereles FS, Passman R, Song G, Kadish AH, Goldberger JJ. Infarct morphology identifies patients with substrate for sustained ventricular tachycardia. *J Am Coll Cardiol* 2005; **45**: 1104-1108

49 **Schmidt A**, Azevedo CF, Cheng A, Gupta SN, Bluemke DA, Foo TK, Gerstenblith G, Weiss RG, Marbán E, Tomaselli GF, Lima JA, Wu KC. Infarct tissue heterogeneity by magnetic resonance imaging identifies enhanced cardiac arrhythmia susceptibility in patients with left ventricular dysfunction. *Circulation* 2007; **115**: 2006-2014

50 **Dickfeld T**, Tian J, Ahmad G, Jimenez A, Turgeman A, Kuk R, Peters M, Saliaris A, Saba M, Shorofsky S, Jeudy J. MRI-Guided ventricular tachycardia ablation: integration of late gadolinium-enhanced 3D scar in patients with implantable cardioverter-defibrillators. *Circ Arrhythm Electrophysiol* 2011;

4: 172-184
51 **van Dockum WG**, ten Cate FJ, ten Berg JM, Beek AM, Twisk JW, Vos J, Hofman MB, Visser CA, van Rossum AC. Myocardial infarction after percutaneous transluminal septal myocardial ablation in hypertrophic obstructive cardiomyopathy: evaluation by contrast-enhanced magnetic resonance imaging. *J Am Coll Cardiol* 2004; **43**: 27-34
52 **Schalla S**, Saeed M, Higgins CB, Weber O, Martin A, Moore P. Balloon sizing and transcatheter closure of acute atrial septal defects guided by magnetic resonance fluoroscopy: assessment and validation in a large animal model. *J Magn Reson Imaging* 2005; **21**: 204-211
53 **Allen KB**, Dowling RD, Fudge TL, Schoettle GP, Selinger SL, Gangahar DM, Angell WW, Petracek MR, Shaar CJ, O'Neill WW. Comparison of transmyocardial revascularization with medical therapy in patients with refractory angina. *N Engl J Med* 1999; **341**: 1029-1036
54 **Ruel M**, Laham RJ, Parker JA, Post MJ, Ware JA, Simons M, Sellke FW. Long-term effects of surgical angiogenic therapy with fibroblast growth factor 2 protein. *J Thorac Cardiovasc Surg* 2002; **124**: 28-34
55 **Stamm C**, Kleine HD, Choi YH, Dunkelmann S, Lauffs JA, Lorenzen B, David A, Liebold A, Nienaber C, Zurakowski D, Freund M, Steinhoff G. Intramyocardial delivery of CD133+ bone marrow cells and coronary artery bypass grafting for chronic ischemic heart disease: safety and efficacy studies. *J Thorac Cardiovasc Surg* 2007; **133**: 717-725
56 **Vulliet PR**, Greeley M, Halloran SM, MacDonald KA, Kittleson MD. Intra-coronary arterial injection of mesenchymal stromal cells and microinfarction in dogs. *Lancet* 2004; **363**: 783-784
57 **Saeed M**, Hetts SW, Do L, Wilson MW. MRI study on volume effects of coronary emboli on myocardial function, perfusion and viability. *Int J Cardiol* 2011; Epub ahead of print
58 **Saeed M**, Hetts SW, Ursell PC, Do L, Kolli KP, Wilson MW. Evaluation of the acute effects of distal coronary microembolization using multidetector computed tomography and magnetic resonance imaging. *Magn Reson Med* 2011; Epub ahead of print
59 **Maintz D**, Ozgun M, Hoffmeier A, Fischbach R, Kim WY, Stuber M, Manning WJ, Heindel W, Botnar RM. Selective coronary artery plaque visualization and differentiation by contrast-enhanced inversion prepared MRI. *Eur Heart J* 2006; **27**: 1732-1736
60 **Yeon SB**, Sabir A, Clouse M, Martinezclark PO, Peters DC, Hauser TH, Gibson CM, Nezafat R, Maintz D, Manning WJ, Botnar RM. Delayed-enhancement cardiovascular magnetic resonance coronary artery wall imaging: comparison with multislice computed tomography and quantitative coronary angiography. *J Am Coll Cardiol* 2007; **50**: 441-447
61 **von Bary C**, Makowski M, Preissel A, Keithahn A, Warley A, Spuentrup E, Buecker A, Lazewatsky J, Cesati R, Onthank D, Schickl N, Schachoff S, Hausleiter J, Schömig A, Schwaiger M, Robinson S, Botnar R. MRI of coronary wall remodeling in a swine model of coronary injury using an elastin-binding contrast agent. *Circ Cardiovasc Imaging* 2011; **4**: 147-155
62 **Brasselet C**, Durand E, Addad F, Al Haj Zen A, Smeets MB, Laurent-Maquin D, Bouthors S, Bellon G, de Kleijn D, Godeau G, Garnotel R, Gogly B, Lafont A. Collagen and elastin cross-linking: a mechanism of constrictive remodeling after arterial injury. *Am J Physiol Heart Circ Physiol* 2005; **289**: H2228-H2233
63 **Saeed M**, Saloner D, Do L, Wilson M, Martin A. Cardiovascular magnetic resonance imaging in delivering and evaluating the efficacy of hepatocyte growth factor gene in chronic infarct scar. *Cardiovasc Revasc Med* 2011; **12**: 111-122
64 **Dick AJ**, Lederman RJ. MRI-guided myocardial cell therapy. *Int J Cardiovasc Intervent* 2005; **7**: 165-170
65 **Baklanov DV**, Demuinck ED, Thompson CA, Pearlman JD. Novel double contrast MRI technique for intramyocardial detection of percutaneously transplanted autologous cells. *Magn Reson Med* 2004; **52**: 1438-1442
66 **Graham JJ**, Foltz WD, Vaags AK, Ward MR, Yang Y, Connelly KA, Vijayaraghavan R, Detsky JS, Hough MR, Stewart DJ, Wright GA, Dick AJ. Long-term tracking of bone marrow progenitor cells following intracoronary injection post-myocardial infarction in swine using MRI. *Am J Physiol Heart Circ Physiol* 2010; **299**: H125-H133
67 **Perin EC**, Dohmann HF, Borojevic R, Silva SA, Sousa AL, Mesquita CT, Rossi MI, Carvalho AC, Dutra HS, Dohmann HJ, Silva GV, Belém L, Vivacqua R, Rangel FO, Esporcatte R, Geng YJ, Vaughn WK, Assad JA, Mesquita ET, Willerson JT. Transendocardial, autologous bone marrow cell transplantation for severe, chronic ischemic heart failure. *Circulation* 2003; **107**: 2294-2302
68 **Assmus B**, Honold J, Schächinger V, Britten MB, Fischer-Rasokat U, Lehmann R, Teupe C, Pistorius K, Martin H, Abolmaali ND, Tonn T, Dimmeler S, Zeiher AM. Transcoronary transplantation of progenitor cells after myocardial infarction. *N Engl J Med* 2006; **355**: 1222-1232
69 **Menasché P**, Alfieri O, Janssens S, McKenna W, Reichenspurner H, Trinquart L, Vilquin JT, Marolleau JP, Seymour B, Larghero J, Lake S, Chatellier G, Solomon S, Desnos M, Hagège AA. The Myoblast Autologous Grafting in Ischemic Cardiomyopathy (MAGIC) trial: first randomized placebo-controlled study of myoblast transplantation. *Circulation* 2008; **117**: 1189-1200
70 **Narazaki G**, Uosaki H, Teranishi M, Okita K, Kim B, Matsuoka S, Yamanaka S, Yamashita JK. Directed and systematic differentiation of cardiovascular cells from mouse induced pluripotent stem cells. *Circulation* 2008; **118**: 498-506
71 **Pearlman JD**, Hibberd MG, Chuang ML, Harada K, Lopez JJ, Gladstone SR, Friedman M, Sellke FW, Simons M. Magnetic resonance mapping demonstrates benefits of VEGF-induced myocardial angiogenesis. *Nat Med* 1995; **1**: 1085-1089
72 **Saeed M**, Saloner D, Martin A, Do L, Weber O, Ursell PC, Jacquier A, Lee R, Higgins CB. Adeno-associated viral vector-encoding vascular endothelial growth factor gene: effect on cardiovascular MR perfusion and infarct resorption measurements in swine. *Radiology* 2007; **243**: 451-460
73 **Omary RA**, Green JD, Fang WS, Viohl I, Finn JP, Li D. Use of internal coils for independent and direct MR imaging-guided endovascular device tracking. *J Vasc Interv Radiol* 2003; **14**: 247-254
74 **Omary RA**, Green JD, Schirf BE, Li Y, Finn JP, Li D. Real-time magnetic resonance imaging-guided coronary catheterization in swine. *Circulation* 2003; **107**: 2656-2659
75 **Serfaty JM**, Yang X, Aksit P, Quick HH, Solaiyappan M, Atalar E. Toward MRI-guided coronary catheterization: visualization of guiding catheters, guidewires, and anatomy in real time. *J Magn Reson Imaging* 2000; **12**: 590-594
76 **Paetzel C**, Zorger N, Bachthaler M, Hamer OW, Stehr A, Feuerbach S, Lenhart M, Völk M, Herold T, Kasprzak P, Nitz WR. Magnetic resonance-guided percutaneous angioplasty of femoral and popliteal artery stenoses using real-time imaging and intra-arterial contrast-enhanced magnetic resonance angiography. *Invest Radiol* 2005; **40**: 257-262
77 **Jeziorska M**, Woolley DE. Local neovascularization and cellular composition within vulnerable regions of atherosclerotic plaques of human carotid arteries. *J Pathol* 1999; **188**: 189-196
78 **Kerwin WF**, Paz O. Cardiac resynchronization therapy: overcoming ventricular dyssynchrony in dilated heart failure. *Cardiol Rev* 2003; **11**: 221-239
79 **Hill JM**, Dick AJ, Raman VK, Thompson RB, Yu ZX, Hinds KA, Pessanha BS, Guttman MA, Varney TR, Martin BJ, Dunbar CE, McVeigh ER, Lederman RJ. Serial cardiac magnetic resonance imaging of injected mesenchymal stem cells. *Circulation* 2003; **108**: 1009-1014
80 **Kraitchman DL**, Tatsumi M, Gilson WD, Ishimori T, Kedzio-

rek D, Walczak P, Segars WP, Chen HH, Fritzges D, Izbudak I, Young RG, Marcelino M, Pittenger MF, Solaiyappan M, Boston RC, Tsui BM, Wahl RL, Bulte JW. Dynamic imaging of allogeneic mesenchymal stem cells trafficking to myocardial infarction. *Circulation* 2005; **112**: 1451-1461

81 **Amsalem Y**, Mardor Y, Feinberg MS, Landa N, Miller L, Daniels D, Ocherashvilli A, Holbova R, Yosef O, Barbash IM, Leor J. Iron-oxide labeling and outcome of transplanted mesenchymal stem cells in the infarcted myocardium. *Circulation* 2007; **116**: I38-I45

82 **Carr CA**, Stuckey DJ, Tatton L, Tyler DJ, Hale SJ, Sweeney D, Schneider JE, Martin-Rendon E, Radda GK, Harding SE, Watt SM, Clarke K. Bone marrow-derived stromal cells home to and remain in the infarcted rat heart but fail to improve function: an in vivo cine-MRI study. *Am J Physiol Heart Circ Physiol* 2008; **295**: H533-H542

83 **Himes N**, Min JY, Lee R, Brown C, Shea J, Huang X, Xiao YF, Morgan JP, Burstein D, Oettgen P. In vivo MRI of embryonic stem cells in a mouse model of myocardial infarction. *Magn Reson Med* 2004; **52**: 1214-1219

84 **Cahill KS**, Germain S, Byrne BJ, Walter GA. Non-invasive analysis of myoblast transplants in rodent cardiac muscle. *Int J Cardiovasc Imaging* 2004; **20**: 593-598

85 **Modo M**, Beech JS, Meade TJ, Williams SC, Price J. A chronic 1 year assessment of MRI contrast agent-labelled neural stem cell transplants in stroke. *Neuroimage* 2009; **47** Suppl 2: T133-T142

86 **Bulte JW**, Kraitchman DL. Monitoring cell therapy using iron oxide MR contrast agents. *Curr Pharm Biotechnol* 2004; **5**: 567-584

87 **Frank JA**, Miller BR, Arbab AS, Zywicke HA, Jordan EK, Lewis BK, Bryant LH, Bulte JW. Clinically applicable labeling of mammalian and stem cells by combining superparamagnetic iron oxides and transfection agents. *Radiology* 2003; **228**: 480-487

88 **Wöhrle J**, Merkle N, Mailänder V, Nusser T, Schauwecker P, von Scheidt F, Schwarz K, Bommer M, Wiesneth M, Schrezenmeier H, Hombach V. Results of intracoronary stem cell therapy after acute myocardial infarction. *Am J Cardiol* 2010; **105**: 804-812

89 **Sardella G**, Mancone M, Bucciarelli-Ducci C, Agati L, Scardala R, Carbone I, Francone M, Di Roma A, Benedetti G, Conti G, Fedele F. Thrombus aspiration during primary percutaneous coronary intervention improves myocardial reperfusion and reduces infarct size: the EXPIRA (thrombectomy with export catheter in infarct-related artery during primary percutaneous coronary intervention) prospective, randomized trial. *J Am Coll Cardiol* 2009; **53**: 309-315

S- Editor Cheng JX **L- Editor** O'Neill M **E- Editor** Zheng XM